Solid State Nuclear Magnetic Resonance **22**, 1–18 (2002)
doi:10.1006/snmr.2002.0053

Solid Echo in the Slow-Motion Region. Effects of the Finite Pulse Widths

P. Bilski,* N. A. Sergeev,[†,1] and J. Wąsicki*

**Faculty of Physics, Adam Mickiewicz University, 61-614 Poznań, Poland; and [†]Institute of Physics, University of Szczecin, 70-451 Szczecin, Poland*

Received June 19, 2001; revised December 18, 2001

The effects of nonzero radio-frequency pulse widths on the echo signals in solids with molecular motions have been investigated. It has been shown that in the slow-motion region a time position and an amplitude of the echo signal depend not only on the width of the pulse, but also on the shape of potential wells and the correlation time, describing the molecular motion. A comparison of the developed theory with experimental results obtained for polycrystalline NH_4Cl demonstrates a good agreement between them. © 2002 Elsevier Science (USA)

Key Words: solid-echo signal; finite width RF pulses; molecular motions.

1. INTRODUCTION

At the present time the "solid-echo" technique $90^{\circ}_{Y} - \tau - 90^{\circ}_{x} - Acq(t)$ [1, 2] is a powerful, NMR method for studying molecular structure and dynamics in solid state. A general review of an application of the deuterium solid-echo technique has been recently published [3, 4]. There are also a great number of papers describing ^1H "solid-echo" technique and its application in a study of molecular dynamics in solids and polymers [4–28]. In almost all of the papers radio-frequency (RF) pulses were assumed to be described by delta-functions (that supposes that $\omega_1 t_{1,2} = \pi/2$ at the pulse length $t_{1,2} \to 0$ and the amplitude of RF field $\omega_1 \to \infty$), so the dipolar interaction Hamiltonian could be omitted during the action of RF pulses. This approximation is not good enough for solids where the experimental RF pulse amplitudes are comparable with dipolar interactions of nuclei. The effects of the width of the hard RF pulses on the solid echoes in solids with rigid lattice have been discussed in a few papers [24–26]. It has been shown that the dipolar interactions of the nuclei during the hard RF pulses produce a shift of the echo signal maximum from the time $t = 2\tau$ and the maximum of the echo signal is observed at $t = 2\tau + t_2 - t_1/2$ [24–26].

In the present paper, we consider the effects of the dipolar spin interaction during the RF pulses on the solid-echo signal for the case, where there are the molecular motions in solids. The preliminary results of our considerations have been already published [27, 28].

[1] To whom correspondence should be addressed. E-mail: sergeev@uoo.univ.szczecin.pl.

0926-2040/02 $35.00

2. THEORY

Let us consider an ensemble of nuclear spins in a high static magnetic field $\mathbf{B}_0$ ($\mathbf{B}_0 \| OZ$). The equilibrium density operator ρ at $t = 0$ can be written in the high-temperature approximation as [29–31]

$$\rho(0) = \beta I_z. \tag{1}$$

Here $\beta = \hbar\omega_0/kT)[Tr(E)]^{-1}$ and E is the unit operator, $\omega_0 = \gamma B_0$ is the Larmor frequency (γ is the magnetogyric ratio of the nuclei) and T is the temperature of a lattice.

If at time $t = 0$, the first RF pulse is applied along the OY-axis in the rotating frame, the evolution of the density operator is described by the Liouville equation [29–31]:

$$i\frac{d\rho}{dt} = [H(t), \rho], \tag{2}$$

where the Hamiltonian $H(t)$ has the form

$$H(t) = -\omega_1 I_Y + H_0(t). \tag{3}$$

Here $\omega_1 = \gamma B_1$ is the amplitude of the RF field and $H_0(t)$ is an interaction Hamiltonian of the ensemble of nuclear spins in the rotating coordinate frame [29–31]. A rotation of the spin frame about the OY-axis with angular velocity ω_1 "removes" the term $(-\omega_1 I_Y)$ from Eq. (3) and equation of motion for the density operator in this new rotating frame has the form

$$i\frac{d\rho_1}{dt} = [H_1, \rho_1]. \tag{4}$$

Here

$$\rho_1(t) = \exp(i\omega_1 t I_Y)\rho(t)\exp(i\omega_1 t I_Y), \tag{5}$$

and

$$H_1(t) = \exp(-i\omega_1 t I_Y)H_0(t)\exp(i\omega_1 t I_Y). \tag{6}$$

The formal solution of Eq. (4) may be written as [29–31]

$$\rho_1(t_1) = \rho_1(0) - i\int_0^{t_1} [H_1(t'), \rho_1(0)]\,dt'$$

$$- \int_0^{t_1} dt'' \int_0^{t''} [H_1(t''), [H_1(t'), \rho_1(0)]]\,dt' + \cdots. \tag{7}$$

Here t_1 is the width of the first RF pulse. If we assume that it is 90°-pulse ($\omega_1 t_1 = \pi/2$), then from Eqs. (7) and (5) we have

$$\rho(t_1) = \beta\left\{ I_X - i\int_0^{t_1} [H_2(t'), I_X]\, dt' - \int_0^{t_1} dt'' \int_0^{t''} [H_2(t''), [H_2(t'), I_X]]\, dt' + \cdots \right\}. \tag{8}$$

Here

$$H_2(t) = \exp\left(i\frac{\pi}{2} I_Y\right) H_1(t) \exp\left(-i\frac{\pi}{2} I_Y\right)$$
$$\equiv \exp\left(i\frac{\pi}{2} I_Y\right) \exp(-i\omega_1 t I_Y) H_0(t) \exp(i\omega_1 t I_Y) \exp\left(-i\frac{\pi}{2} I_Y\right). \tag{9}$$

After the first RF pulse, the free evolution of the density operator is described by the interaction Hamiltonian $H_0(t)$ in the rotating coordinate frame and at time τ (the time τ is measured from the beginning of the first pulse) the density operator has the form

$$\rho(\tau, t_1) = \rho(t_1) - i\int_{t_1}^{\tau} [H_0(t'), \rho(t_1)]\, dt' - \int_{t_1}^{\tau} dt'' \int_{t_1}^{t''} [H_0(t''), [H_0(t'), \rho(t_1)]]\, dt' + \cdots. \tag{10}$$

Inserting Eq. (8) into Eq. (10) we have

$$\rho(\tau, t_1) = \beta\left\{ I_X - i\int_0^{t_1} [H_2(t'), I_X]\, dt' - \int_0^{t_1} dt'' \int_0^{t''} [H_2(t''), [H_2(t'), I_X]]\, dt' - i\int_{t_1}^{\tau} [H_0(t'), I_X]\, dt' - \int_{t_1}^{\tau} dt'' \int_0^{t_1} [H_0(t''), [H_2(t'), I_X]]\, dt' - \int_{t_1}^{\tau} dt'' \int_{t_1}^{t''} [H_0(t''), [H_0(t'), I_X]]\, dt' + \cdots \right\}. \tag{11}$$

If at time τ the second 90°-RF pulse ($\omega_1 t_2 = \pi/2$, t_2 is the width of the second RF pulse) is applied along the OX-axis in the rotating frame, the density operator becomes

$$\rho(t_2, \tau, t_1) = \rho_2(\tau, t_1) - i\int_{\tau}^{\tau+t_2} [H_4(t'), \rho_2(\tau, t_1)]\, dt' - \int_{\tau}^{\tau+t_2} dt'' \int_{\tau}^{t''} [H_4(t''), [H_4(t'), \rho_2(\tau, t_1)]]\, dt' + \cdots. \tag{12}$$

Here

$$\rho_2(\tau, t_1) = \beta\Bigg\{ I_X - i\int_0^{t_1} [H_5(t'), I_X]\, dt' - \int_0^{t_1} dt'' \int_0^{t''} [H_5(t''), [H_5(t'), I_X]]\, dt' - i\int_{t_1}^{\tau} [H_3(t'), I_X]\, dt' - \int_{t_1}^{\tau} dt'' \int_0^{t_1} [[H_3(t''), [H_5(t'), I_X]]\, dt' - \int_{t_1}^{\tau} dt'' \int_{t_1}^{t''} [H_3(t''), [H_3(t'), I_X]]\, dt' + \cdots \Bigg\}, \tag{13}$$

where

$$H_3(t) = \exp\left(i\frac{\pi}{2} I_X\right) H_0(t) \exp\left(-i\frac{\pi}{2} I_X\right), \tag{14}$$

$$H_4(t) = \exp\left(i\frac{\pi}{2} I_X\right) \exp(-i\omega_1 t I_X) H_0(t) \exp(i\omega_1 t I_X) \exp\left(-i\frac{\pi}{2} I_X\right), \tag{15}$$

and

$$H_5(t) = \exp\left(i\frac{\pi}{2} I_X\right) H_2(t) \exp\left(-i\frac{\pi}{2} I_X\right). \tag{16}$$

Inserting Eq. (13) into Eq. (12) we obtain

$$\rho(t_2, \tau, t_1) = \beta\Bigg\{ I_X - i\int_0^{t_1} [H_5(t'), I_X]\, dt' - \int_0^{t_1} dt'' \int_0^{t''} [H_5(t''), [H_5(t'), I_X]]\, dt' - i\int_{t_1}^{\tau} [H_3(t'), I_X]\, dt' - \int_{t_1}^{\tau} dt'' \int_0^{t_1} [H_3(t''), [H_5(t'), I_X]]\, dt' - \int_{t_1}^{\tau} dt'' \int_{t_1}^{t''} [H_3(t''), [H_3(t'), I_X]]\, dt' - \int_{\tau}^{\tau+t_2} dt'' \int_0^{t_1} [H_4(t''), [H_5(t'), I_X]]\, dt' - \int_{\tau}^{\tau+t_2} dt'' \int_{t_1}^{\tau} [H_4(t''), [H_3(t'), I_X]]\, dt' - \int_{\tau}^{\tau+t_2} dt'' \int_{\tau}^{t''} [H_4(t''), [H_4(t'), I_X]]\, dt' + \cdots \Bigg\}. \tag{17}$$

After the second RF pulse the free evolution of the density operator is described by the interaction Hamiltonian $H_0(t)$ and at time t (the time t is measured from the beginning of the first pulse) the density operator has the form

$$\rho(t,t_2,\tau,t_1)=\rho(t_2,\tau,t_1)-i\int_{\tau+t_2}^{t}[H_0(t'),\rho(t_2,\tau,t_1)]\,dt' - \int_{\tau+t_2}^{t}dt''\int_{\tau+t_2}^{t''}[H_0(t''),[H_0(t'),\rho(t_2,\tau,t_1)]]\,dt'. \tag{18}$$

Inserting Eq. (17) into Eq. (18), we obtain

$$\begin{aligned}\rho(t,t_2,\tau,t_1)=\beta'\Bigg\{&I_X-i\int_0^{t_1}[H_5(t'),I_X]\,dt'-\int_0^{t_1}dt''\int_0^{t''}[H_5(t''),[H_5(t'),I_X]]\,dt'\\
&-i\int_{t_1}^{\tau}[H_3(t'),I_X]\,dt'-\int_{t_1}^{\tau}dt''\int_0^{t_1}[H_3(t''),[H_5(t'),I_X]]\,dt'\\
&-\int_{t_1}^{\tau}dt''\int_0^{t''}[H_3(t''),[H_3(t'),I_X]]\,dt'\\
&-\int_{\tau}^{\tau+t_2}dt''\int_0^{t_1}[H_4(t''),[H_5(t'),I_X]]\,dt'\\
&-\int_{\tau}^{\tau+t_2}dt''\int_{t_1}^{\tau}[H_4(t''),[H_3(t'),I_X]]\,dt'\\
&-\int_{\tau}^{\tau+t_2}dt''\int_{\tau}^{t''}[H_4(t''),[H_4(t'),I_X]]\,dt'\\
&-\int_{\tau+t_2}^{t}dt''\int_0^{t_1}[H_0(t''),[H_5(t'),I_X]]\,dt'\\
&-\int_{\tau+t_2}^{t}dt''\int_{t_1}^{\tau}[H_0(t''),[H_3(t'),I_X]]\,dt'\\
&-\int_{\tau+t_2}^{t}dt''\int_{\tau+t_2}^{t''}[H_0(t''),[H_0(t'),I_X]]\,dt'+\cdots\Bigg\}.\end{aligned} \tag{19}$$

The observed transient response of the ensemble of spins on the two-pulse signal, is proportional to the expected value of the X-component of spin operator [29–31]

$$V(t,t_2,\tau,t_1)\propto\frac{Tr\{\overline{\rho(t,t_2,\tau,t_1)}I_X\}}{Tr(I_X^2)}, \tag{20}$$

where the upper bar denotes the average of the density operator on the random motions of the nuclei.

Substituting Eq. (19) into Eq. (20) we obtain

$$
\begin{aligned}
V(t,t_2,\tau,t_1) \propto \frac{\beta}{Tr(I_X^2)}\Bigg\{ & Tr(I_X^2) - i\int_0^{t_1} Tr\{I_X\overline{[H_5(t'),I_X]}\}\,dt' \\
& - \int_0^{t_1} dt'' \int_0^{t''} Tr\{I_X\overline{[H_5(t''),[H_5(t'),I_X]]}\}\,dt' \\
& - i\int_{t_1}^{\tau} Tr\{I_X\overline{[H_3(t'),I_X]}\}\,dt' \\
& - \int_{t_1}^{\tau} dt'' \int_0^{t_1} Tr\{I_X\overline{[H_3(t''),[H_5(t'),I_X]]}\}\,dt' \\
& - \int_{t_1}^{\tau} dt'' \int_{t_1}^{t''} Tr\{I_X\overline{[H_3(t''),[H_3(t'),I_X]]}\}\,dt' \\
& - \int_{\tau}^{\tau+t_2} dt'' \int_0^{t_1} Tr\{I_X\overline{[H_4(t''),[H_5(t'),I_X]]}\}\,dt' \\
& - \int_{\tau}^{\tau+t_2} dt'' \int_{t_1}^{\tau} Tr\{I_X\overline{[H_4(t''),[H_3(t'),I_X]]}\}\,dt' \\
& - \int_{\tau}^{\tau+t_2} dt'' \int_{\tau}^{t''} Tr\{I_X\overline{[H_4(t''),[H_4(t'),I_X]]}\}\,dt' \\
& - \int_{\tau+t_2}^{t} dt'' \int_0^{t_1} Tr\{I_X\overline{[H_0(t''),[H_5(t'),I_X]]}\}\,dt' \\
& - \int_{\tau+t_2}^{t} dt'' \int_{t_1}^{\tau} Tr\{I_X\overline{[H_0(t''),[H_3(t'),I_X]]}\}\,dt' \\
& - \int_{\tau+t_2}^{t} dt'' \int_{\tau+t_2}^{t''} Tr\{I_X\overline{[H_0(t''),[H_0(t'),I_X]]}\}\,dt' + \cdots \Bigg\}. \qquad (21)
\end{aligned}
$$

Hereafter, we will consider only secular terms of the interactions Hamiltonians: $H_0(t)$, $H_1(t)$, $H_2(t)$, $H_3(t)$ and $H_4(t)$, $H_5(t)$ [29–31]. This approach is equivalent to the first approximation of the perturbation theory and it is fulfilled if the RF pulses are the hard RF pulses ($\omega_1 \gg \|H_0\|$) [29–31].

The secular part of the Hamiltonian $H_0(t)$ has the form [29]

$$H_0(t) \equiv H_z(t) + H_{IS}(t), \qquad (22a)$$

where

$$H_z(t) = \sum_{i>k} b_{ik}(t)(2I_{iZ}I_{kZ} - I_{iY}I_{kY} - I_{iX}I_{kX}), \qquad (22b)$$

$$H_{IS}(t) = \sum_{i,\alpha} c_{i\alpha}(t) I_{iZ} S_{\alpha Z}. \tag{22c}$$

In Eqs. (22b) and (22c),

$$b_{ik}(t) = \frac{\mu_0 \hbar}{8\pi} \gamma_I^2 R_{ik}^{-3} (1 - 3\cos^2 \vartheta_{ik}), \tag{23}$$

$$c_{i\alpha}(t) = \frac{\mu_0 \hbar}{4\pi} \gamma_I \gamma_S R_{i\alpha}^{-3} (1 - 3\cos^2 \vartheta_{i\alpha}), \tag{24}$$

where μ_0 is the permeability of vacuum, ϑ_{ik} is the angle between the vector $\mathbf{R}_{ik}$ (the subscripts i and k denote the resonant nuclei) and external magnetic field $\mathbf{B}_0$, $\vartheta_{i\alpha}$ is the angle between the vector $\mathbf{R}_{i\alpha}$ (the subscript α denotes nonresonant nuclei) and external magnetic field $\mathbf{B}_0$. $H_0(t)$ is explicitly time-dependent through the time dependence of the functions $b_{ik}(t)$ and $c_{i\alpha}(t)$.

As it results from Eqs. (6), (9), (16) and (22) the secular parts of the Hamiltonians $H_1(t)$, $H_2(t)$ and $H_5(t)$ are as follows:

$$\begin{aligned} H_1(t) &= H_2(t) \\ &= -\frac{1}{2} \sum_{i>k} b_{ik}(t)(2I_{iY}I_{kY} - I_{iZ}I_{kZ} - I_{iX}I_{kX}) \equiv -\frac{1}{2} H_Y, \end{aligned} \tag{25}$$

$$H_5(t) = -\frac{1}{2} \sum_{i>k} b_{ik}(t)(2I_{iZ}I_{kZ} - I_{iY}I_{kY} - I_{iX}I_{kX}) \equiv -\frac{1}{2} H_Z. \tag{26}$$

Similarly, from Eqs. (14), (15) and (22) one can extract the secular parts of the Hamiltonian $H_3(t)$ and $H_4(t)$:

$$H_3(t) = \sum_{i>k} b_{ik}(t)(2I_{iY}I_{kY} - I_{iZ}I_{kZ} - I_{iX}I_{kX}) + \sum_{i,\beta} c_{i\alpha}(t) I_{iY} S_{\alpha Z}, \tag{27}$$

$$H_4(t) = \frac{1}{2} \sum_{i>k} b_{ik}(t)(2I_{iX}I_{kX} - I_{iZ}I_{kZ} - I_{iY}I_{kY}) \equiv -\frac{1}{2} H_X(t). \tag{28}$$

Inserting Eqs. (25) and (26) into Eq. (21) we obtain

$$\begin{aligned} V(t, t_2, \tau, t_1) = \frac{\beta}{Tr(I_X^2)} \cdot \Bigg\{ & Tr(I_X^2) - \frac{1}{4} \int_0^{t_1} dt'' \int_0^{t''} Tr\{I_X \overline{[H_Z(t''), [H_Z(t'), I_X]]}\}\, dt' \\ & + \frac{1}{2} \int_{t_1}^{\tau} dt'' \int_0^{t_1} Tr\{I_X \overline{[H_Y(t''), [H_Z(t'), I_X]]}\}\, dt' \end{aligned}$$

$$
\begin{aligned}
&- \int_{t_1}^{\tau} dt'' \int_{t_1}^{t''} Tr\{I_X \overline{[H_Y(t''), [H_Y(t'), I_X]]}\}\, dt' \\
&+ \frac{1}{2} \int_{\tau+t_2}^{t} dt'' \int_{0}^{t_1} Tr\{I_X \overline{[H_Z(t''), [H_Z(t'), I_X]]}\}\, dt' \\
&- \int_{\tau+t_2}^{t} dt'' \int_{t_1}^{\tau} Tr\{I_X \overline{[H_Z(t''), [H_Y(t'), I_X]]}\}\, dt' \\
&- \int_{\tau+t_2}^{t} dt'' \int_{\tau+t_2}^{t''} Tr\{I_X \overline{[H_Z(t''), [H_Z(t'), I_X]]}\}\, dt' \\
&- \int_{t_1}^{\tau} dt'' \int_{t_1}^{t''} Tr\{I_X \overline{[H_{IS}(t''), [H_{IS}(t'), I_X]]}\}\, dt' \\
&- \int_{\tau+t_2}^{t} dt'' \int_{t_1}^{\tau} Tr\{I_X \overline{[H_{IS}(t''), [H_{IS}(t'), I_X]]}\}\, dt' \\
&- \int_{\tau+t_2}^{t} dt'' \int_{\tau+t_2}^{t''} Tr\{I_X \overline{[H_{IS}(t''), [H_{IS}(t'), I_X]]}\}\, dt' + \cdots \Bigg\}. \qquad (29)
\end{aligned}
$$

Evaluating the traces in Eq. (29) we have

$$
\begin{aligned}
V(t, t_2, \tau, t_1) = \beta \cdot \Bigg[& 1 - \frac{1}{4} \int_0^{t_1} dt'' \int_0^{t''} h(t'', t')\, dt' - \frac{1}{2} \int_{t_1}^{\tau} dt'' \int_0^{t_1} h(t'', t')\, dt' \\
& - \int_{t_1}^{\tau} dt'' \int_{t_1}^{t''} h(t'', t')\, dt' + \frac{1}{2} \int_{\tau+t_2}^{t} dt'' \int_0^{t_1} h(t'', t')\, dt' \\
& + \int_{\tau+t_2}^{t} dt'' \int_{t_1}^{\tau} h(t'', t')\, dt' - \int_{\tau+t_2}^{t} dt'' \int_{\tau+t_2}^{t''} h(t'', t')\, dt' \\
& - \int_{t_1}^{\tau} dt'' \int_{t_1}^{t''} g(t'', t')\, dt' \\
& - \int_{\tau+t_2}^{t} dt'' \int_{t_1}^{\tau} g(t'', t')\, dt' - \int_{\tau+t_2}^{t} dt'' \int_{\tau+t_2}^{t''} g(t'', t')\, dt'' + \cdots \Bigg]. \qquad (30)
\end{aligned}
$$

Here

$$
h(t'', t') = W_1 \sum_{i,k} \overline{a_{ik}(t'') a_{ik}(t')}, \qquad (31)
$$

$$
g(t'', t') = W_2 \sum_{i,\alpha} \overline{d_{i\alpha}(t'') d_{i\alpha}(t')} \qquad (32)
$$

are the correlation functions of the dipolar local field [29–31].

In Eqs. (31) and (32):

$$W_1 = \frac{3}{4}\left(\frac{\mu_0}{4\pi}\right)^2 \gamma^4 \hbar^2 I(I+1)\frac{1}{N}, \quad a_{ik}(t') = R_{ik}^{-3}(t')[1 - 3\cos^2\theta_{ik}(t')], \tag{33}$$

$$W_2 = \frac{1}{3}\left(\frac{\mu_0}{4\pi}\right)^2 \gamma_I^2 \gamma_S^2 \hbar^2 S(S+1)\frac{1}{N}, \quad d_{ij}(t') = R_{i\alpha}^{-3}(t')[1 - 3\cos^2\theta_{i\alpha}(t')]. \tag{34}$$

First, we have considered the case of "rigid" lattice, with no molecular motions in the crystal. For this case, we obtain from Eqs. (31) and (32) as follows:

$$h(0,0) = W_1 \sum_{i,k} a_{ik}^2 = M_{2II}, \tag{35a}$$

$$g(0,0) = W_2 \sum_{i,\alpha} d_{i\alpha}^2 = M_{2IS}. \tag{35b}$$

In Eqs. (35a) and (35b), M_{2II} and M_{2IS} are the homo- and heteronuclear contributions to the second moment of the NMR line, respectively.

Inserting Eqs. (35a) and (35b) into Eq. (30) and calculating integrals we obtain the well-known result [32, 33]:

$$V(t, t_2, \tau, t_1) = \beta[1 - \tfrac{1}{2}M_{2II}(t - 2\tau - t_2 + \tfrac{1}{2}t_1)^2 - \tfrac{1}{2}M_{2IS}(t - t_1 - t_2)^2 + \cdots]. \tag{36}$$

In the case of the fast motion region, when correlation functions $h(t'', t')$, $g(t'', t')$ do not depend on time, one obtains

$$h(0,0) = W_1 \sum_{i,k} \bar{a}_{ik}^2 = \bar{M}_{2II}, \tag{37}$$

$$g(0,0) = W_2 \sum_{i,\alpha} \bar{d}_{i\alpha}^2 = \bar{M}_{2IS}, \tag{38}$$

In Eqs. (37) and (38), $\bar{M}_{2II}$ and $\bar{M}_{2IS}$ are the homo- and heteronuclear contributions to the second moment of motionally narrowed NMR line, respectively [29, 34].

Inserting Eqs. (37) and (38) into Eq. (30) and calculating integrals we again obtain the well-known result:

$$V(t, t_2, \tau, t_1) = \beta[1 - \tfrac{1}{2}\bar{M}_{2II}(t - 2\tau - t_2 + \tfrac{1}{2}t_1)^2 - \tfrac{1}{2}\bar{M}_{2IS}(t - t_1 - t_2)^2 + \cdots]. \tag{39}$$

From Eqs. (36) and (39) it follows that only homonuclear dipolar interactions generate the solid-echo signal. Therefore, we should further consider only homonuclear spin systems. It is worth noting that in the case of the stationary stochastical process the correlation functions $h(t'', t')$ and $g(t'', t')$ depend only on $z = |t'' - t'| > 0$.

In this case we can write Eq. (30) as

$$
\begin{aligned}
V(t,t_2,\tau,t_1) = \beta\Bigg[1 &- \frac{1}{4}\int_0^{t_1}(t_1 - z)h(z)\,dz - \frac{1}{2}\int_0^{t_1} zh(z)\,dz \\
&- \frac{t_1}{2}\int_{t_1}^{\tau-t_1} h(z)\,dz - \frac{1}{2}\int_{\tau-t_1}^{\tau}(\tau - z)h(z)\,dz \\
&- \int_0^{\tau-t_1}[(\tau - t_1) - z]h(z)\,dz \\
&- \frac{1}{2}\int_{\tau+t_2-t_1}^{\tau+t_2}[(\tau + t_2 - t_1) - z]h(z)\,dz + \frac{t_1}{2}\int_{\tau+t_2}^{t-t_1} h(z)\,dz \\
&+ \frac{1}{2}\int_{t-t_1}^{t}(t - z)h(z)\,dz - \int_{t_2}^{\tau+t_2-t_1}(t_2 - z)h(z)\,dz \\
&+ (\tau - t_1)\int_{\tau+t_2-t_1}^{t-\tau} h(z)\,dz + \int_{t-\tau}^{t-t_1}[(t - t_1) - z]h(z)\,dz \\
&- \int_0^{t-\tau-t_2}[(t - \tau - t_2) - z]h(z)\,dz + \cdots\Bigg].
\end{aligned}
\tag{40}
$$

2.1. *Molecular Motions between Equivalent Potential Wells*

In order to calculate the correlation function $h(z)$ we consider the simple model of the molecular motion of resonant nuclei between the equivalent potential wells determined in crystal lattice by discrete lattice sites Ω_l $(l = 1,2,\ldots,n)$ [34]. We assume that the process of the random molecular motions in solids is the stationary Markov process. For this case the correlation function $h(z)$ is given by [27, 34]

$$
h(z) = \bar{M}_{2II} + \Delta M_{2II}\exp\left(-\frac{z}{\tau_c}\right), \tag{41}
$$

where

$$
\Delta M_{2II} = M_{2II} - \bar{M}_{2II} \tag{42}
$$

and τ_c is the correlation time, characterizing molecular motion.

Using the correlation function (41) and calculating the integrals in Eq. (40) we obtain

$$
\begin{aligned}
V(t,t_2,\tau,t_1) = \beta\Bigg\{1 &- \frac{1}{2}\bar{M}_{2II}\left[t - \left(2\tau + t_2 - \frac{t_1}{2}\right)\right]^2 \\
&- \Delta M_{2II}\tau_c^2 R(t,t_2,\tau,t_1,\tau_c) + \cdots\Bigg\},
\end{aligned}
\tag{43}
$$

where

$$R(t,t_2,\tau,t_1,\tau_c) = -\frac{7}{4}+\frac{t}{\tau_c}-\frac{3t_1}{4\tau_c}-\frac{t_2}{\tau_c}-\frac{1}{4}\exp\left(-\frac{t_1}{\tau_c}\right)-\exp\left(-\frac{t_2}{\tau_c}\right)$$
$$-\frac{1}{2}\exp\left(-\frac{t}{\tau_c}\right)+\frac{1}{2}\exp\left(-\frac{\tau-t_1}{\tau_c}\right)-\frac{1}{2}\exp\left(-\frac{t-t_1}{\tau_c}\right)$$
$$+\frac{1}{2}\exp\left(-\frac{\tau+t_2}{\tau_c}\right)+\exp\left(-\frac{t-\tau}{\tau_c}\right)+\exp\left(-\frac{t-\tau-t_2}{\tau_c}\right)$$
$$+\frac{1}{2}\exp\left(-\frac{\tau}{\tau_c}\right)+\frac{1}{2}\exp\left(-\frac{\tau+t_2-t_1}{\tau_c}\right)\Bigg]. \tag{44}$$

In the case of the polycrystalline sample we must average Eq. (43) over all possible orientations of the crystallites. If we denote the averaged values of $\bar{M}_{2II}$ and ΔM_{2II} as $\langle\bar{M}_{2II}\rangle$ and $\langle\Delta M_{2II}\rangle$, then for small τ and t we can write

$$V(t,t_2,\tau,t_1) = \beta\Bigg\{1-\frac{1}{2}\langle\bar{M}_{2II}\rangle\left[t-\left(2\tau+t_2-\frac{t_1}{2}\right)\right]^2$$
$$-\langle\Delta M_{2II}\rangle\tau_c^2 R(t,t_2,\tau,t_1,\tau_c)+\cdots\Bigg\}$$
$$\approx\frac{\hbar\omega_0}{kT}\exp\Bigg\{-\frac{1}{2}\langle\bar{M}_{2II}\rangle\left[t-\left(2\tau+t_2-\frac{t_1}{2}\right)\right]^2$$
$$-\langle\Delta M_{2II}\rangle\tau_c^2 R(t,t_2,\tau,t_1,\tau_c)\Bigg\}. \tag{45}$$

The temperature dependence of the amplitude and the time position of the solid echo are shown in Fig. 1a and b. From Fig. 1a it follows that the temperature dependence of solid-echo amplitude slightly depends on the RF pulses width. From Fig. 1b it follows that time position of the solid-echo maximum depends on the RF pulses width, as well as on the correlation time τ_c of the molecular motion. The dramatic changes in the solid-echo behavior are observed in the slow-motion region ($\langle M_{2II}\rangle \tau_c^2 \approx 1$), where the amplitude of the solid-echo signal is reduced and the maximum of the echo signal is shifted to the end of the second pulse.

2.2. Molecular Motions between the Nonequivalent Potential Sites

In the case of molecular motion between the nonequivalent potential wells, the correlation function $h(z)$ may be written as [35–38]

$$h(z) = K_0 + \sum_{i\neq 0} K_i \exp\left(-\frac{z}{\tau_{ci}}\right). \tag{46}$$

Here K_j ($j = 0, 1, 2, \ldots, n$) are the structural parameters, dependent on the shape of the potential well and τ_{ci} are the correlation times, characterizing n modes of reorientation [35–38].

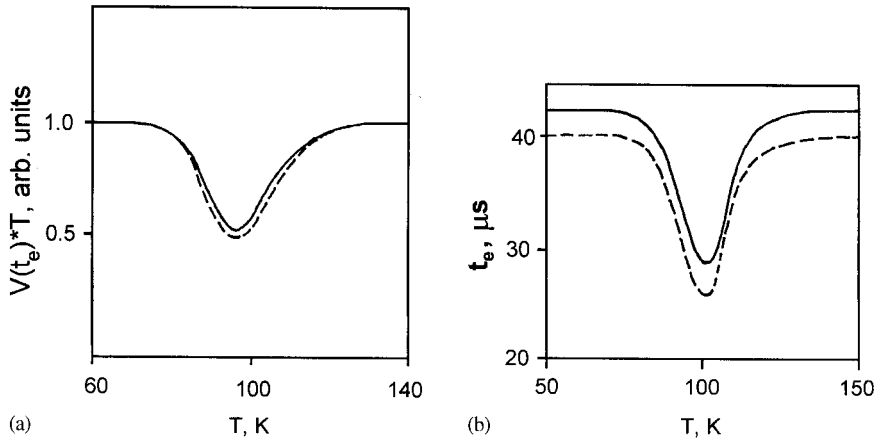

FIG. 1. (a) The temperature dependence of the $V(t_e) \times T$ calculated from Eq. (45) using the following parameters: $\tau = 20$ μs; $M_{2II} = 8 \times 10^{-3}$ rad μs^{-2}, $\tilde{M}_{2II} = 10^{-3}$ rad μs^{-2}; $\tau_c = 10^{-14}$ exp(16.6 kJ mol^{-1}/RT) s; - - -, $t_1 = t_2 = 0$ μs; ——, $t_1 = t_2 = 5$ μs. (b) The temperature dependence of the time position t_e of the maximum solid echo calculated from Eq. (45) using the following parameters: $M_{2II} = 8 \times 10^{-3}$ rad μs^{-2}, $M_{2II} = 10^{-3}$ rad μs^{-2}; $\tau_c = 10^{-14}$ exp(16.6 kJ mol^{-1}/RT) s; $\tau = 20$ μs; - - -, $t_1 = t_2 = 0$ μs; ——, $t_1 = t_2 = 5$ μs.

Using the correlation function (46), we obtain from Eq. (40)

$$V(t, t_2, \tau, t_1) = \beta\left\{1 - \frac{1}{2}K_0\left[t - \left(2\tau + t_2 - \frac{t_1}{2}\right)\right]^2 \cdot \right. \\ \left. - \sum_{i \neq 0} K_i \tau_{ci}^2 R_i(t, t_2, \tau, t_1, \tau_{ci}) + \cdots\right\}, \tag{47}$$

where

$$R_i(t, t_2, \tau, t_1, \tau_{ci}) = -\frac{7}{4} + \frac{t}{\tau_{ci}} - \frac{3t_1}{4\tau_{ci}} - \frac{t_2}{\tau_{ci}} - \frac{1}{4}\exp\left(-\frac{t_1}{\tau_{ci}}\right) - \exp\left(-\frac{t_2}{\tau_{ci}}\right) \\ - \frac{1}{2}\exp\left(-\frac{t}{\tau_{ci}}\right) + \frac{1}{2}\exp\left(-\frac{\tau - t_1}{\tau_{ci}}\right) - \frac{1}{2}\exp\left(\frac{t - t_1}{\tau_{ci}}\right) \\ + \frac{1}{2}\exp\left(-\frac{\tau + t_2}{\tau_{ci}}\right) + \exp\left(-\frac{t - \tau}{\tau_{ci}}\right) + \exp\left(-\frac{t - \tau - t_2}{\tau_{ci}}\right) \\ + \frac{1}{2}\exp\left(-\frac{\tau}{\tau_{ci}}\right) + \frac{1}{2}\exp\left(-\frac{\tau + t_2 - t_1}{\tau_{ci}}\right)\Bigg]. \tag{48}$$

The temperature dependences of the amplitude and the time position of the solid echo signal for the different potentials considered in [35] are shown in Figs. 2(a, b)–5(a, b). The structural parameters K_i ($i = 0, 1, 2, \ldots, n$) and the correlation times τ_{ci} for different shape of the potential well, are defined as follows [35]:

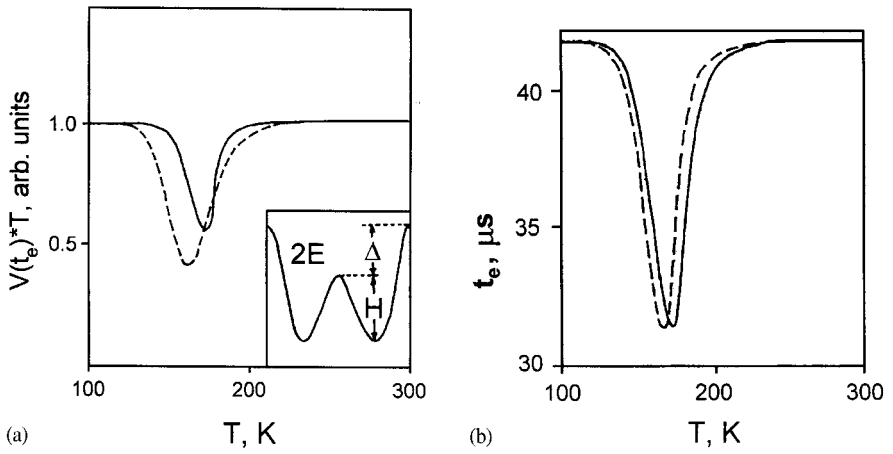

FIG. 2. (a) Main plot: the temperature dependence of the $V(t_e) \times T$ calculated from Eq. (47) for $2E$-shape of the potential well, using the following parameters: $M_{2II} = 8 \times 10^{-3}$ rad μs^{-2}; $\tau_0 = 10^{-14}$ s; $H = 29$ kJ mol^{-1}; $t_1 = t_2 = 3.6$ μs; $\tau = 20$ μs; ——, $\Delta = 14.5$ kJ mol^{-1}; - - -, $\Delta = 0$ kJ mol^{-1}. Inset: schematic representation of the $2E$-potential well. (b) The temperature dependence of the time position t_e of the maximum solid echo calculated from Eq. (47) for $2E$-shape of the potential well, using the following parameters: $M_{2II} = 8 \times 10^{-3}$ rad μs^{-2}; $\tau_0 = 10^{-14}$ s, $H = 29$ kJ mol^{-1}; $t_1 = t_2 = 3.6$ μs, $\tau = 20$ μs; ——, $\Delta = 14.5$ kJ mol^{-1}; - - -, $\Delta = 0$ kJ mol^{-1}.

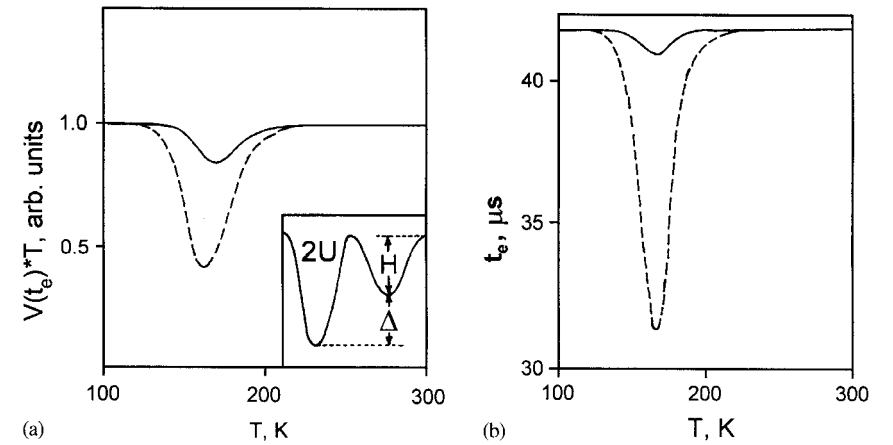

FIG. 3. (a) Main plot: the temperature dependence of the $V(t_e) \times T$ calculated from Eq. (47) for $2U$-shape of the potential well, using the following parameters: $M_{2II} = 8 \times 10^{-3}$ rad μs^{-2}; $\tau_0 = 10^{-14}$ s, $H = 29$ kJ mol^{-1}; $t_1 = t_2 = 3.6$ μs, $\tau = 20$ μs; ——, $\Delta = 14.5$ kJ mol^{-1}; - - -, $\Delta = 0$ kJ mol^{-1}. Inset: schematic representation of the $2U$-potential well. (b) The temperature dependence of the time position t_e of the maximum solid echo calculated from Eq. (47) for $2U$-shape of the potential well, using the following parameters: $M_{2II} = 8 \times 10^{-3}$ rad μs^{-2}; $\tau_0 = 10^{-14}$ s, $H = 29$ kJ mol^{-1}; $t_1 = t_2 = 3.6$ μs, $\tau = 20$ μs; ——, $\Delta = 4.5$ kJ mol^{-1}; - - -, $\Delta = 0$ kJ mol^{-1}.

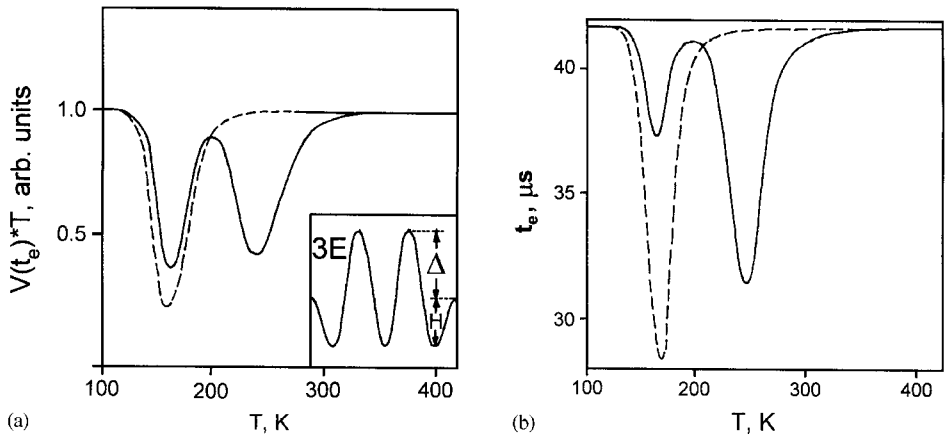

FIG. 4. (a) Main plot: the temperature dependence of the $V(t_e) \times T$ calculated from Eq. (47) for $3E$-shape of the potential well, using the following parameters: $M_{2II} = 8 \times 10^{-3}$ rad μs^{-2}; $\tau_0 = 10^{-14}$ s, $H = 29$ kJ mol^{-1}; $t_1 = t_2 = 3.6$ μs, $\tau = 20$ μs; ——, $\Delta = 14.5$ kJ mol^{-1}; - - -, $\Delta = 0$ kJ mol^{-1}. Inset: schematic representation of the $3E$-potential well. (b) The temperature dependence of the time position t_e of the maximum solid echo calculated from Eq. (47) for $3E$-shape of the potential well, using the following parameters: $\Delta M_{2II} = 8 \times 10^{-3}$ rad μs^{-2}; $\tau_0 = 10^{-14}$ s, $H = 29$ kJ mol^{-1}; $t_1 = t_2 = 3.6$ μs, $\tau = 20$ μs; ——, $\Delta = 14.5$ kJ mol^{-1}; - - -, $\Delta = 0$ kJ mol^{-1}.

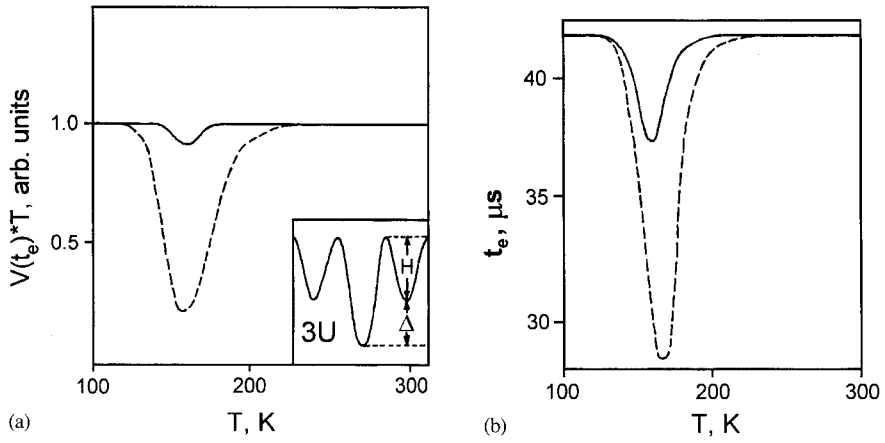

FIG. 5. (a) Main plot: the temperature dependence of the $V(t_e) \times T$ calculated from Eq. (47) for $3U$-shape of the potential well, using the following parameters: $M_{2II} = 8 \times 10^{-3}$ rad μs^{-2}; $\tau_0 = 10^{-14}$ s, $H = 29$ kJ mol^{-1}; $t_1 = t_2 = 3.6$ μs, $\tau = 20$ μs; ——, $\Delta = 14.5$ kJ mol^{-1}; - - -, $\Delta = 0$ kJ mol^{-1}. Inset: schematic representation of the $3U$ potential well. (b) The temperature dependence of the time position t_e of the maximum solid echo calculated from Eq. (47) for $3U$-shape of the potential well, using the following parameters: $\Delta M_{2II} = 8 \times 10^{-3}$ rad/μs^{-2}; $\tau_0 = 10^{-14}$ s, $H = 29$ kJ mol^{-1}; $t_1 = t_2 = 3.6$ μs, $\tau = 20$ μs; ——, $\Delta = 14.5$ kJ mol^{-1}; - - -, $\Delta = 0$ kJ mol^{-1}.

2E-potential well:

$$K_0 = \tfrac{1}{4}M_{2II}, \qquad K_1 = \tfrac{3}{4}M_{2II},$$

$$\tau_{c1} = \frac{a}{1+a}\tau_0 \exp\left(\frac{H}{RT}\right), \qquad a = \exp\left(\frac{\Delta}{RT}\right).$$

2U-potential well:

$$K_0 = M_{2II}\left[1 - \frac{3a}{(1+a)^2}\right], \qquad K_1 = \frac{3a}{(1+a)^2}M_{2II},$$

$$\tau_{c1} = \frac{a}{1+a}\tau_0 \exp\left(\frac{H}{RT}\right), \qquad a = \exp\left(\frac{H}{RT}\right).$$

3E-potential well:

$$K_0 = \tfrac{1}{4}M_{2II}, \qquad K_1 = K_2 = \tfrac{3}{8}M_{2II},$$

$$\tau_{c1} = \frac{a}{3}\tau_0 \exp\left(\frac{H}{RT}\right), \qquad \tau_{c2} = \frac{a}{1+2a}\tau_0 \exp\left(\frac{H}{RT}\right), \qquad a = \exp\left(\frac{\Delta}{RT}\right).$$

3U-potential well:

$$K_0 = M_{2II}\left[1 - \frac{27}{8}\frac{a}{(a+2)^2} - \frac{9}{8(a+2)}\right], \qquad K_1 = M_{2II}\frac{27a}{8(a+2)^2},$$
$$K_2 = M_{2II}\frac{9}{8(a+2)},$$

$$\tau_{c1} = \frac{a}{a+2}\tau_0 \exp\left(\frac{H}{RT}\right), \qquad \tau_{c2} = \frac{1}{3}\tau_0 \exp\left(\frac{H}{RT}\right), \qquad a = \exp\left(\frac{\Delta}{RT}\right).$$

The parameters H and Δ characterizing the $2E$, $2U$, $3E$ and $3U$ potential wells are defined on insets of Figs. 2a–5a.

From Fig. 2 one can see that, as in the case of NMR second moment [35], the temperature dependence of the solid-echo amplitude for $2E$ well is almost independent of Δ. On the contrary, for $2U$ and $3U$ potential wells, it strongly depends on Δ. The interesting dependence of the solid-echo amplitude on temperature is observed for $3E$-potential well. For this case the two well-resolved minima are observed. The temperature at which the low-temperature minimum is observed depends on the energy H, while the temperature at which the high-temperature minimum takes place is determined by the energy $H + \Delta$.

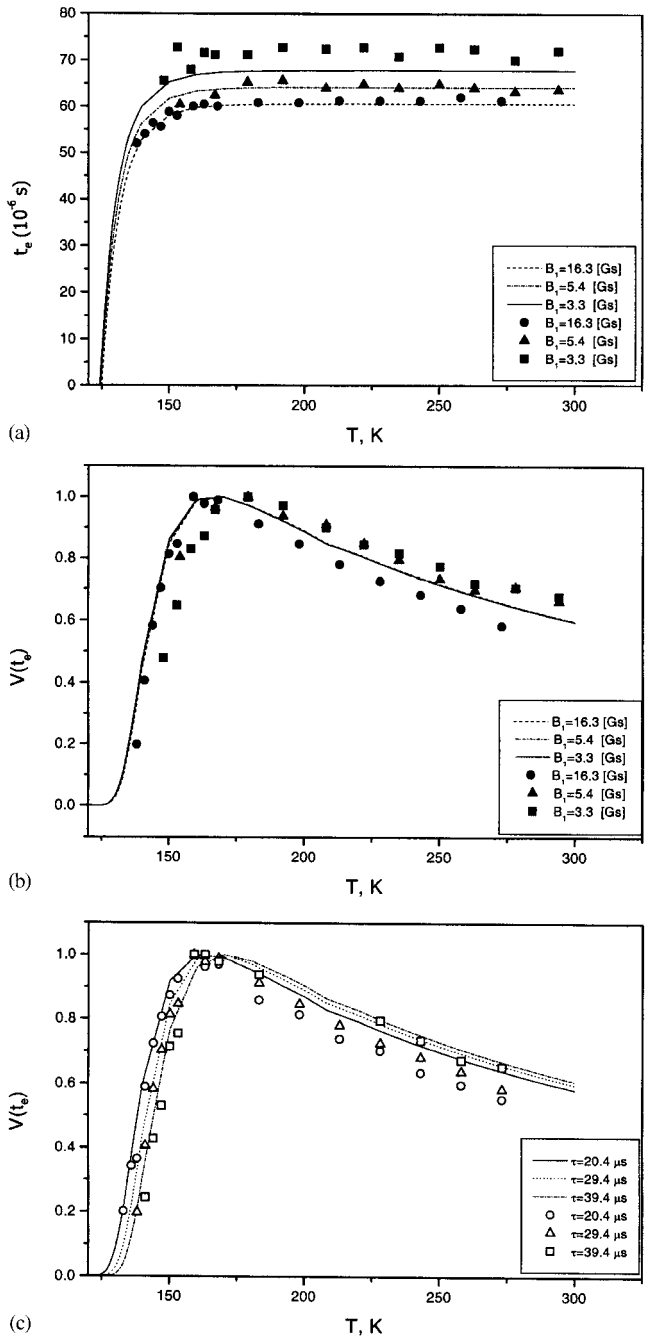

FIG. 6. (a) The temperature dependence of the time position t_e of the maximum solid-echo amplitude for polycrystalline NH_4Cl at different values of RF field, $\tau = 29.4$ μs. (b) The temperature dependence of the maximum solid-echo amplitude $V(t_e)$ for polycrystalline NH_4Cl at different values of RF field, $\tau = 29.4$ μs. (c) The temperature dependence of the maximum solid-echo amplitude $V(t_e)$ for polycrystalline NH_4Cl at different values of pulse spacing, $B_1 = 16.3$ G s.

3. EXPERIMENTAL RESULTS AND DISCUSSION

The theoretical results obtained have been applied to the analysis of temperature dependences of the solid-echo signals observed in polycrystalline ammonium chloride (NH_4Cl). It is now well established that in NH_4Cl there are the reorientations of the ammonium ions about three- and two-fold symmetry axes [39].

^1H NMR experiments were performed on the pulse spectrometer operating at 60 MHz, in the temperature range from 133 to 273 K.

The experimental results of the maximum echo time position (t_e) at different pulse spacing and at different values of RF field obtained for polycrystalline NH_4Cl as a function of temperature are shown in Fig. 6a. One can see that for any pulse spacing the maximum of two-pulse signal does not depend on the temperature, for $T > 160$ K. The maximum of the echo signal is observed at $t_e \approx 2\tau + t_2 - t_1/2$. At $T < 160$ K the time position of the maximum of the echo signal is shifted to the end of the second pulse and the echo signal disappears. The solid and broken lines in Fig. 6a are the theoretical curves for the time positions of the echo maximum, as calculated from Eq. (45) using the results of the relaxation studies of these compounds [39]. For NH_4Cl we have used the following parameters: $\tau_c = (2.16 \times 10^{-14}\ \text{s}) \exp(19.85\ \text{kJ mol}^{-1}/RT)$; $\langle \overline{M_{2II}} \rangle = 4.74 \times 10^{-8}\ \text{T}^2$; $\langle \overline{\Delta M_{2II}} \rangle = 46.15 \times 10^{-8}\ \text{T}^2$. The agreement between theory and experiment is quite reasonable, especially since no parameters have been adjusted.

The experimental results of the maximum echo amplitude at different values of RF field and different pulse spacing as a function of temperature, are shown in Fig. 6b and c. In all the cases, the plotted points were normalized so that the maximum value of the echo amplitude was set equal to 1.0. The solid lines in Fig. 6b and c are the theoretical curves obtained from Eq. (45) using the same parameters as for the theoretical curves in Fig. 6a. From these figures one can see that the developed theory describes rather well the observed temperature dependences of the echo amplitude.

4. CONCLUSIONS

From our consideration it follows that time position and amplitude of the solid-echo maximum depend on the correlation time τ_c of molecular motion, and on the width of RF pulses. The dramatical changes in the solid-echo behavior are observed in the slow-motion region ($\langle M_{2II} \rangle \tau_c^2 \approx 1$), where the amplitude of the solid-echo signal is reduced and the maximum of the echo signal is shifted to the end of the second pulse. We have shown that in the slow-motion region the time position and amplitude of the solid echo are sensitive to the details and thermal parameters of molecular dynamic process. It has also been shown that the study of the temperature dependence of the time position and amplitude of the solid-echo maximum can yield valuable information about the shape of the potential wells in solids.

REFERENCES

1. J. G. Powles and P. Mansfield, *Phys. Rev. Lett.* **2**, 58 (1962).
2. J. G. Powles and J. H. Strange, *Proc. Phys. Soc.* **82**, 7 (1963).

3. G. L. Hoatson and R. L. Vold, "NMR Basic Principles and Progress," Vol. 32, pp. 1–67, Springer-Verlag, Berlin, Heidelberg, 1994.
4. R. R. Vold, *in* "Nuclear Magnetic Resonance Probes of Molecular Dynamics" (R. Tycko, Ed.), pp. 27–112, Kluwer Academic Publishers, Dordrecht, Netherlands, 1994.
5. H. W. Spiess and H. Sillescu, *J. Magn. Res.* **42**, 381 (1981).
6. T. B. Smith, E. A. Moore, and M. Mortimer, *J. Phys. C* **14**, 3965 (1981).
7. N. A. Sergeev, D. S. Ryabushkin, and Yu. N. Moskvich, *Phys. Lett. A* **104**, 97 (1984).
8. A. Baram, *J. Phys. Chem.* **88**, 1695 (1984).
9. T. B. Smith, *Phys. Lett. A* **108**, 295 (1985).
10. M. Mortimer, G. Oates, and T. B. Smith, *Chem. Phys. Lett.* **115**, 299 (1985).
11. D. S. Ryabushkin, Yu. N. Moskvich, and N. A. Sergeev, *Phys. Lett. A* **121**, 357 (1987).
12. M. S. Greenfield, A. D. Ronemus, R. L. Vold, and R. R. Vold, *J. Magn. Res.* **72**, 89 (1987).
13. N. A. Sergeev, D. S. Ryabushkin, and N. P. Kolpaschikova, *Phys. Lett.* **152**, 87 (1991).
14. P. Bilski, N. A. Sergeev, and J. Wąsicki, *in* "Materiały XXXI Ogólnopolskiego Seminarium NMR" (J. Hennel, Ed.), pp. 139–142, IFJ PAN, Kraków, 1999.
15. J.-P. Cohen-Addad, *J. Chem. Phys.* **60**, 2440 (1974).
16. J.-P. Cohen-Addad, *J. Chem. Phys.* **63**, 4880 (1975).
17. J.-P. Cohen-Addad, *J. Phys. (Paris)* **43**, 1509 (1982).
18. J.-P. Cohen-Addad, M. Domard, and J. Herz, *J. Chem. Phys.* **76**, 2744 (1982).
19. J.-P. Cohen-Addad, *Prog. Nucl. Magn. Res. Spectrosc.* **25**, 1 (1993).
20. J. Collignon, H. Sillescu, and H. W. Spiess, *Colloid Polym. Sci.* **259**, 220 (1981).
21. J. Collignon and H. Sillescu, *J. Polym. Sci., Polym. Lett. Ed.* **18**, 669 (1980).
22. P. T. Callaghan and E. T. Samulski, *Macromolecules* **30**, 113 (1997).
23. R. C. Ball, P. T. Callaghan and E. T. Samulski, *J. Chem. Phys.* **106**, 7352 (1997).
24. M. Bloom, J. H. Davis, and M. I. Valic, *Can. J. Phys.* **58**, 1510 (1980).
25. P. M. Henrichs, J. M. Hewitt, and M. Linder, *J. Magn. Res.* **60**, 280 (1984).
26. N. A. Sergeev, *Solid State NMR* **10**, 45 (1997).
27. P. Bilski, N. A. Sergeev, and J. Wasicki, *Appl. Magn. Res.* **18**, 115 (2000).
28. P. Bilski, N. A. Sergeev, and J. Wąsicki, *Mol. Phys. Rep. (Poland)* **29**, 57 (2000).
29. A. Abragam, "The Principles of Nuclear Magnetism," Clarendon Press, Oxford, 1961.
30. M. Mehring, "Principles of High Resolution NMR in Solids," Springer, Berlin, 1983.
31. R. R. Ernst, G. Bodenhausen, and A. Wokaun, "Principles of NMR in One and Two Dimensions," Oxford Scientific, Oxford, 1987.
32. P. Mansfield, *Phys. Rev. A* **137**, 961 (1965).
33. N. Boden, M. Gibb, Y. K. Levine, and M. Mortimer, *J. Magn. Res.* **16**, 471 (1974).
34. C. P. Slichter, "Principles of Magnetic Resonance," Springer, Berlin, 1980.
35. E. R. Andrew and L. Latanowicz, *J. Magn. Res.* **68**, 232 (1986).
36. L. Latanowicz and Z. Pająk, *Mol. Phys.* **82** 1187 (1994).
37. L. Latanowicz, E. R. Andrew, and E. C. Reynhardt, *J. Magn. Res. A* **107**, 195 (1994).
38. A. Kozak, M. Grottel, J. Wąsicki, and Z. Pająk, *Phys. Stat. Sol. A* **141**, 345 (1994).
39. R. Goc and J. Wąsicki, *Z. Naturforsch. A* **52**, 609 (1997).